Effects of target plasma electron-electron collisions on correlated motion of fragmented H_2^+ protons

Manuel D. Barriga-Carrasco
E.T.S.I. Industriales, Universidad de Castilla-La Mancha, E-13071 Ciudad Real, Spain
(Received 28 September 2005; published 2 February 2006)

The objective of the present work is to examined the effects of plasma target electron-electron collisions on H_2^+ protons traversing it. Specifically, the target is deuterium in a plasma state with temperature $T_e=10$ eV and density $n=10^{23}$ cm^{-3}, and proton velocities are $v_p=v_{th}$, $v_p=2v_{th}$, and $v_p=3v_{th}$, where v_{th} is the electron thermal velocity of the target plasma. Proton interactions with plasma electrons are treated by means of the dielectric formalism. The interactions among close protons through plasma electronic medium are called vicinage forces. It is checked that these forces always screen the Coulomb explosions of the two fragmented protons from the same H_2^+ ion decreasing their relative distance. They also align the interproton vector along the motion direction, and increase the energy loss of the two protons at early dwell times while for longer times the energy loss tends to the value of two isolated protons. Nevertheless, vicinage forces and effects are modified by the target electron collisions. These collisions enhance the calculated self-stopping and vicinage forces over the collisionless results. Regarding proton correlated motion, when these collisions are included, the interproton vector along the motion direction overaligns at slower proton velocities ($v_p=v_{th}$) and misaligns for faster ones ($v_p=2v_{th}$, $v_p=3v_{th}$). They also contribute to a great extend to increase the energy loss of the fragmented H_2^+ ion. This later effect is more significant in reducing projectile velocity.

DOI: 10.1103/PhysRevE.73.026401 PACS number(s): 52.40.Mj, 52.65.Yy, 52.20.Fs, 52.25.Mq

I. INTRODUCTION

In recent years, it has been demonstrated that subpicosecond high intensity lasers can generate short bunches of dense ion beams [1–6]. When the density of an atomic beam increases the ions get closer and new interactions take place between them. But these interactions can be also observed in low density molecular ion beams. These ions dissociate when entering the target, so that the resulting charged fragments are very close to each other and their motion is also highly correlated [7–11]. The energy loss of molecular beams being higher than the one of atomic beams, they have also been proposed as drivers for inertial confinement fusion [12,13]. Regardless of the origin of the closeness of the charges, the interaction force between them when they move through an electronic medium (plasma) is called vicinage forces [14]. These vicinage forces change the stopping and give rise to the correlated stopping.

It is known that target electron-electron collisions play an important role in the noncorrelated ion stopping [15], so it is expected that these collisions also play an important role in the ion beam collective stopping. The influence of these electron collisions in correlated ion stopping will be considered through the dielectric formalism. The dielectric formalism has become one of the most used methods to describe the interaction of swift ions and other charged particles with matter. The use of this formalism to study the energy loss of charged particles was introduced by Fermi [16]. Subsequent developments made it possible to extend the dielectric formalism to provide a more comprehensive description of the stopping of ions in matter [17,18]. Large number of calculations of electronic stopping forces of ions and electrons in plasmas have been carried out using the classical random phase approximation (RPA) in the dielectric formalism (see Ref. [19] for a complete list).

However, the RPA predicts an infinite lifetime for electron-electron collisions, whereas it is well known that in real materials these excitations are damped. Although it seems to be a straightforward substitution, the replacement of ω by $\omega+i\nu$ in the RPA dielectric functions where ν represents the collision damping, is erroneous, as it does not conserve the local particle number. Mermin [20] derived an expression for the dielectric function taking account of the finite lifetime of the collisions and also preserving the local particle number.

Dielectric formalism has been successfully applied to the interaction of protons with plasmas [21] and molecular protons beams with solid targets [22]. In this article protons will also be used, as they are the most simple ions upon which one can examine these collision effects. The final purpose of this work is to include our theoretical model in our computer code TAMIM (transport of atomic and molecular ions in matter), formerly known as MBC-ITFIP [23]. There is no doubt that a user friendly computer code can be of great help for the plasma scientific community.

In Sec. II the dielectric formalism used to study the plasma electron-electron collisions is detailed. The influences of these collisions on proton electronic self-stopping and vicinage forces are shown in Sec. III. Then the effects on the correlated motion of the protons are analyzed in Sec. IV.

II. DIELECTRIC FUNCTION

In the dielectric formalism, the target is characterized by its dielectric function $\epsilon(k,\omega)$, which contains relevant information about its response to electronic excitations with momentum k and energy ω. The longitudinal dielectric function of a classical electron plasma in the RPA is [24]

$$\epsilon_{\mathrm{RPA}}(k,\omega) = 1 + \frac{k_D^2}{k^2}[W(\xi) + Y(\xi)], \tag{1}$$

with

$$W(\xi) = 1 - \sqrt{2}\xi \exp(-\xi^2/2)\int_0^{\xi/\sqrt{2}} \exp(-x^2)dx \tag{2}$$

and

$$Y(\xi) = \sqrt{\frac{\pi}{2}}\xi \exp(-\xi^2/2), \tag{3}$$

where $\xi=\omega/(kv_{\mathrm{th}})$ with $v_{\mathrm{th}}=\sqrt{k_BT}$ the electron thermal velocity, $k_D=\omega_p/v_{\mathrm{th}}$ the inverse Debye length, and $\omega_p=\sqrt{4\pi n}$ the plasma frequency in atomic units (a.u.).

As mentioned in the Introduction, the RPA predicts an infinite life for electron-electron collisions, whereas it is well known that in real materials these excitations are damped. So, it is straightforward substituting ω by $\omega+i\nu$ in the RPA dielectric function, obtaining the relaxation time approximation (RTA), where ν represents the collision frequency. This method is erroneous as it does not conserve the local particle number and has not Drude behavior at long wavelengths ($k \to 0$)

$$\epsilon_D(k,\omega) = 1 - \frac{\omega_p^2}{\omega(\omega+i\nu)}. \tag{4}$$

The Mermin dielectric function [20] is derived using an expansion of the local equilibrium distribution function to conserve the local particle number

$$\epsilon_M(k,\omega) = 1 + \frac{(\omega+i\nu)[\epsilon_{\mathrm{RPA}}(k,\omega+i\nu)-1]}{\omega+i\nu[\epsilon_{\mathrm{RPA}}(k,\omega+i\nu)-1]/[\epsilon_{\mathrm{RPA}}(k,0)-1]}, \tag{5}$$

where $\epsilon_{\mathrm{RPA}}(k,\omega+i\nu)$ is the RPA dielectric function in the RTA case. It is easy to see that when $\nu\to 0$, the Mermin dielectric function reproduces the RPA function.

For ion stopping considerations, it is worth defining the energy loss function (ELF)

$$\mathrm{ELF} \equiv \mathrm{Im}\left(\frac{-1}{\epsilon_x(k,\omega)}\right), \tag{6}$$

where $\epsilon_x(k,\omega)$ represents any dielectric function stated before. Figure 1 shows Drude, RTA, and Mermin ELFs dependence with ω/ω_p when $k\to 0$, for a $T_e=10$ eV and $n=10^{23}$ cm^{-3} deuterium plasma. For this plasma, the collision frequency, $\nu=0.225\omega_p$, is obtained from Spitzer [25]. Mermin energy loss function reproduces quite well Drude energy loss function but it is not the case for the RTA one. It means that the collisions are not included correctly in the RTA dielectric function, and so Mermin result will be chosen as the most appropriate one for calculating next self-stopping and vicinage forces.

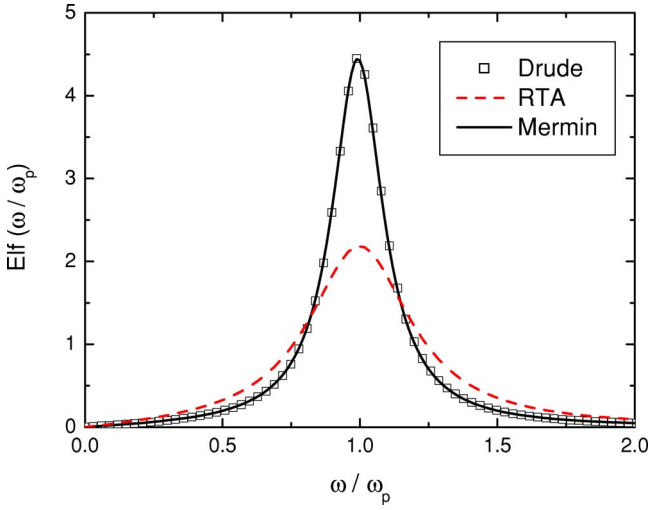

FIG. 1. (Color online) Drude, RTA, and Mermin energy loss functions dependence with ω/ω_p when $k\to 0$, for a $T_e=10$ eV and $n=10^{23}$ cm^{-3} deuterium plasma. The collision frequency is $\nu=0.225\omega_p$.

III. SELF-STOPPING AND VICINAGE ELECTRONIC FORCES

The electronic ion stopping can be divided into the contribution due to itself and the contribution due to its partners. The first one is called self-stopping electronic force and the second one vicinage electronic force. Following the dielectric formalism and using atomic units, the induced force produced by a pointlike charge Z_{p1}, moving at velocity v inside a uniform electron gas, on a neighbor charge Z_{p2} is [26]

$$F_z(z,\sigma) = \frac{2Z_{p1}Z_{p2}}{\pi v_{p1}^2}\int_0^\infty \frac{dk}{k}\int_0^{kv} d\omega\, \omega\, J_0(\sigma\sqrt{k^2-\omega^2/v_{p1}^2}) \times\left\{\sin(\omega z/v_{p1})\mathrm{Re}\left[\frac{1}{\epsilon_x(k,\omega)}-1\right] + \cos(\omega z/v_{p1})\mathrm{Im}\left[\frac{1}{\epsilon_x(k,\omega)}-1\right]\right\}, \tag{7}$$

$$F_\sigma(z,\sigma) = \frac{2Z_{p1}Z_{p2}}{\pi v_{p1}}\int_0^\infty \frac{dk}{k}\int_0^{kv} d\omega\, J_1(\sigma\sqrt{k^2-\omega^2/v_{p1}^2}) \times\sqrt{k^2-\omega^2/v_{p1}^2}\left\{\cos(\omega z/v_{p1})\mathrm{Re}\left[\frac{1}{\epsilon_x(k,\omega)}-1\right] - \sin(\omega z/v_{p1})\mathrm{Im}\left[\frac{1}{\epsilon_x(k,\omega)}-1\right]\right\}, \tag{8}$$

where z and σ are the coordinates parallel and perpendicular of the neighbor projectile from the projectile that generates the potential in the reference frame of the motion of the last one. $J_0(x)$ and $J_1(x)$ are the zeroth and the first order Bessel functions. It is worthwhile to mention that the induced or vicinage forces in Eqs. (7) and (8) do not include the Coulomb force and only depend on the target through its dielectric function $\epsilon_x(k,\omega)$. Figure 2 shows the $F_z(z,\sigma)$ as a function of z that a proton $Z_1=1$ with velocity $v=2.5v_{\mathrm{th}}$ produces

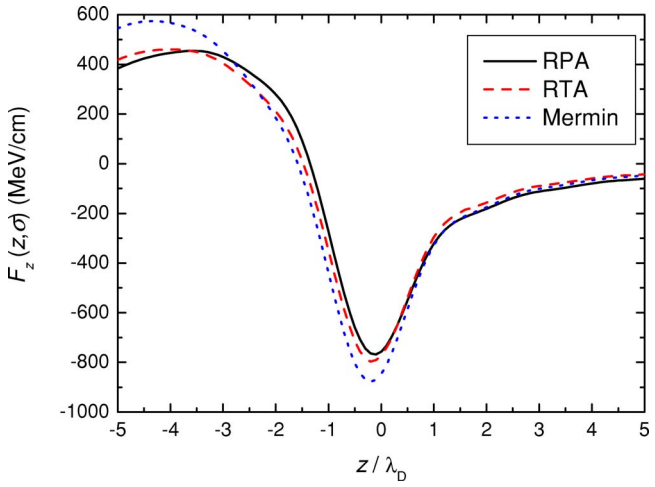

FIG. 2. (Color online) $F_z(z,\sigma)$ as a function of z at $\sigma=0$ that a proton $Z_1=1$ with velocity $v=2.5v_{\text{th}}$ produces on another proton located at $(z,\sigma=0)$. RPA case is compared with the RTA and Mermin cases when $\nu=0.225\omega_p$.

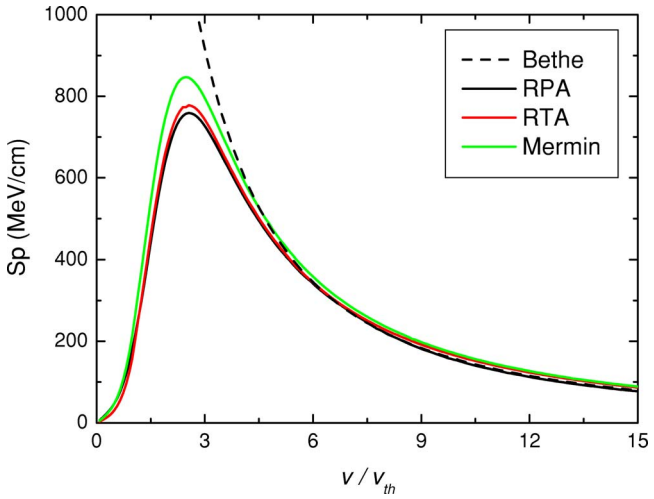

FIG. 3. (Color online) RPA self-stopping ion force as a function of ion velocity in a $T_e=10$ eV and $n=10^{23}$ cm^{-3} plasma compared with the Bethe formula. Self-stopping RTA and Mermin forces are compared with the RPA case using collision frequency $\nu=0.225\omega_p$.

on another proton located at $(z,\sigma=0)$. The RPA case is compared with the RTA and Mermin cases when $\nu=0.225\omega_p$. The modulus of the force $|F_z(z,\sigma)|$ increases when collisions are considered in RTA and Mermin calculations.

Assigning $z=\sigma=0$ and $Z_{p1}=Z_{p2}$ to Eqs. (7) and (8) results $F_\sigma=0$, and F_z yields the self-stopping particle force F_s. The variation of the projectile kinetic energy is $dE=\mathbf{F}_s\mathbf{v}_{p1}dt$ so the electronic stopping S_p defined as the energy loss per unit path length, becomes

$$S_p=\frac{-dE}{v_{p1}\,dt}=-F_{s,z}(z=0,\sigma=0). \tag{9}$$

Then the well-known electronic stopping formula for one projectile is recovered

$$S_p=\frac{2Z_{p1}^2}{\pi v_{p1}^2}\int_0^\infty\frac{dk}{k}\int_0^{kv}d\omega\,\omega\,\text{Im}\left[\frac{-1}{\epsilon_x(k,\omega)}\right]. \tag{10}$$

A cutoff, $k_{\max}=(v_p^2+2v_{\text{th}}^2)/{Z_{p1}}^2$, is introduced to avoid divergence of the k integral in Eqs. (7), (8), and (10). This divergence is caused by inadequacy of the classical treatment of the short-range interactions between the projectile and the plasma electrons [24].

Substituting $\epsilon_x(k,\omega)$ by the corresponding RPA dielectric function, the self-stopping force for the random phase approximation is obtained. Figure 3 represents the self-stopping proton force for the RPA case as a function of ion velocity. It is compared with Bethe result. To examine the effects of the target electron-electron collisions in the self-stopping ion force, the collision frequency ν is included in the dielectric function. RTA case results from changing the $\epsilon_{\text{RPA}}(k,\omega)$ to $\epsilon_{\text{RPA}}(k,\omega+i\nu)$ in Eq. (10). For this target plasma, ν is equal to $0.225\omega_p$. It is seen that this new result is higher than RPA one, meaning that target electron-electron collisions increases self-stopping ion force. Mermin calculation is also included in Fig. 3, showing that this case is higher than the RPA case and it is even higher than the RTA one. The increase due to these collisions in the self-stopping force is more significant at its maximum value.

IV. RESULTS

This section analyzes the effects of considering plasma target electron collisions in the correlated motion of protons from fragmented H_2^+ ions. For this purpose, a numerical code named TAMIM has been developed. This code describes the evolution of the protons inside the plasma by means of a 3D molecular dynamics (MD) simulation, i.e., the trajectory of each proton is followed by integrating the Newton equations of motion with a finite difference algorithm. The forces acting on each proton at each timestep are: the electronic self-stopping force, the reciprocal vicinage forces and the Coulomb repulsion. The interest in the study of the H_2^+ ions is that these ions are composed of two protons, therefore when they dissociate, they can be used to study the correlated motion of very close protons. But the same calculations can be made for more complex molecular ions.

The H_2^+ ion will lose its electron just entering the target and dissociates into two protons $Z_{p1}=Z_{p2}=1$ and $m_p=1$ in proton units (p.u.), separated by an initial distance $r_0=1.08\times10^{-8}$ cm [22]. This yields two protons that move in close proximity, interacting between them and with the target electrons. The target is considered to be deuterium, $Z_n=1$ and $m_n=2$ in p.u., in a plasma state characterized by its density $n=10^{23}$ cm^{-3} and its temperature $T=10$ eV. H_2^+ velocities incident on plasma target are similar to electron thermal velocity $v_p\simeq v_{\text{th}}$.

The main difference on the transport between two correlated or isolated protons is due to Coulomb and vicinage forces. So, it is interesting to analyze how target electron collisions influence two fundamental quantities for calculating these forces: the interproton distance r and the azimuthal angle between the interproton vector and the motion direc-

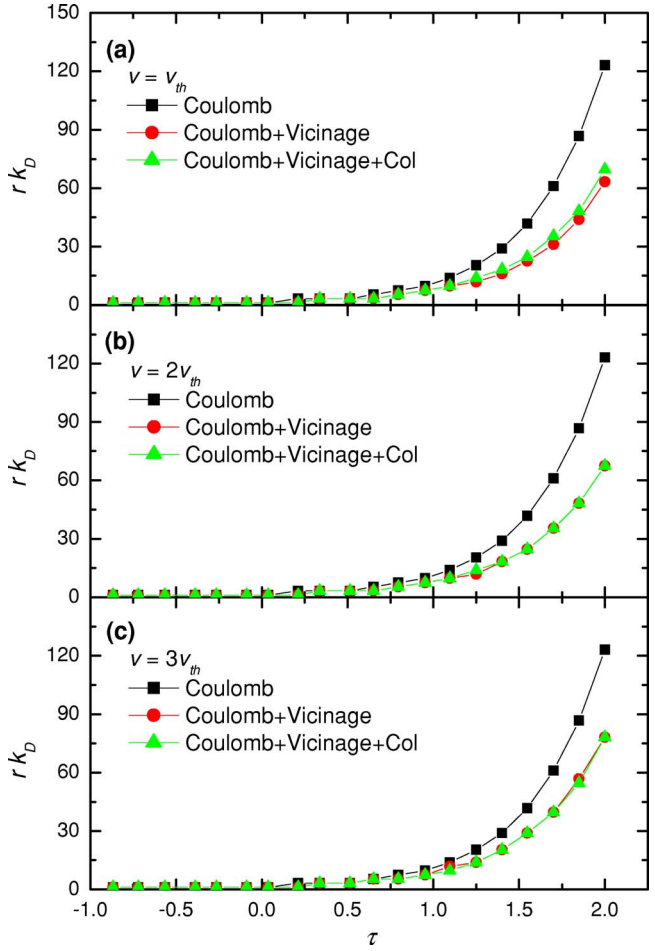

FIG. 4. (Color online) Evolution of the adimensional interproton distance rk_D as a function of the logarithm of dwell time τ during the Coulomb explosion of a H_2^+ ion with the initial angle $\alpha_0=60°$ traversing the plasma with different velocities (a) $v_p=v_{\text{th}}$, (b) $v_p=2v_{\text{th}}$, and (c) $v_p=3v_{\text{th}}$. Each graph represents this evolution taking into account only bare Coulomb force, Coulomb and vicinage forces, and Coulomb force and vicinage forces considering target electron collisions.

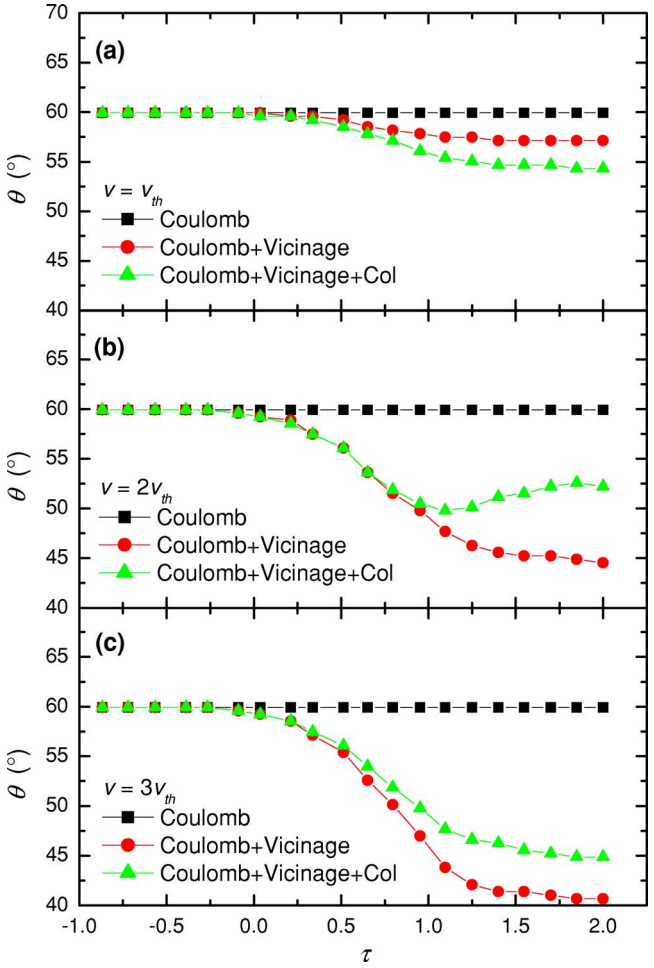

FIG. 5. (Color online) Evolution of α as a function of the logarithm of dwell time τ when the initial azimuthal angle is $\alpha_0=60°$; for the same conditions as in Fig. 4.

tion α. It is appropriate to introduce the logarithm of the dimensionless dwell time (t) $\tau=\log_{10}(t/t_c)$, where t_c is the characteristic Coulomb explosion time of the two protons fragmented from a H_2^+ ion. The characteristic Coulomb explosion time is obtained as $t_c=r_0/u_c=1.47$ fs, where u_c is the asymptotic relative radial velocity of the protons after their bare Coulomb explosion.

Figure 4 displays the evolution of the interproton distance r as a function of the logarithm of dwell time τ during the Coulomb explosion of a H_2^+ ion with the initial angle $\alpha_0=60°$ impacting the plasma target at different velocities (a) $v_p=v_{\text{th}}$, (b) $v_p=2v_{\text{th}}$, and (c) $v_p=3v_{\text{th}}$. Each graph represents the r evolution taking into account only bare Coulomb force, Coulomb and vicinage forces without considering target electron collisions, and Coulomb and vicinage forces considering them. It is seen that vicinage forces always delay Coulomb explosions. This screening is consequence of the asymmetry of the vicinages forces. F_σ is usually negative (see Fig. 2) so it tries to join the two protons in σ direction. F_z is usually negative at small positive z and positive at small negative z (see Fig. 2) so it also approaches the two protons in z direction. It results in decreasing the interproton distance in both σ and z directions and retarding the Coulomb explosion. This is more significant in the late dwell times when the two protons are quite separated out and Coulomb force is smaller than vicinage forces. Also, it can be noticed that Coulomb screening is slightly more relevant at lower speeds meaning that the averaged vicinage force along proton trajectory is more important at lower velocities. Not many changes result when target electron collisions are included in the calculations. Small differences are only noticed for the slowest velocity $v_p=v_{\text{th}}$. Now the Coulomb screening produced by the vicinage forces is smaller than when these collisions are not included. For faster velocities discrepancies between considering or not considering the collisions in computer simulations are not relevant.

Vicinage forces tend to align the interproton vector in the motion direction due to its asymmetry [27]. So next, the influence of target electron collisions in the interproton azimuthal angle α will be examined. Figure 5 represents the α evolution as a function of the logarithm of dwell time τ when the initial azimuthal angle is $\alpha_0=60°$ for the same conditions

as in Fig. 4. When only bare Coulomb forces are considered the azimuthal angle does not vary as expected, but when vicinage forces are added to calculations this angle decreases to indicate that the interproton vector aligns along motion direction. This also results from the asymmetry of the vicinage forces. In this case, angle decreasing means that the alignment power of the F_σ force is higher than the F_z one along protons travel. This effect is not so significant at low velocities as the ratio between F_σ and F_z forces is smaller. When target electron collisions are included in the calculations the interproton overaligns for slowest projectile velocity $v_p = v_{\text{th}}$, while it misaligns for faster velocities. This later misalignment is more relevant for the proton velocity $v_p = 2v_{\text{th}}$.

Finally target electron collisions effects on H_2^+ energy loss are analyzed. If the two fragmented protons are considered as one system, the H_2^+ electronic stopping can be obtained theoretically as the sum of all electronic forces in the $-z$ direction

$$S_{pH_2^+} = 2S_{pH^+} - F_z(z,\sigma) - F_z(-z,\sigma), \tag{11}$$

where S_{pH^+} is the electronic stopping of one isolated proton calculated from Eq. (10). $S_{pH_2^+}$ depends on time through the variation of the coordinates z and σ, at the same time that these coordinates vary due to the Coulomb and vicinage forces. H_2^+ electronic stopping ratio R_2 can be defined to compare the electronic stopping at different projectile incident velocities

$$R_2 = \frac{S_{pH_2^+}}{2S_{pH^+}} = 1 - \frac{F_z(z,\sigma) + F_z(-z,\sigma)}{2S_{pH^+}}. \tag{12}$$

But this ratio can also be calculated directly with our computer code as the ratio between the energy loss of the fragmented H_2^+ ion considering vicinage forces and the energy loss of the fragmented H_2^+ ion without considering vicinage forces, i.e.,

$$R_2 = \frac{\Delta E^*_{H_2^+}}{\Delta E_{H_2^+}}, \tag{13}$$

where $\Delta E^*_{H_2^+}$ and $\Delta E_{H_2^+}$ refers to H_2^+ energy loss with and without vicinage force, respectively.

Figure 6 shows the H_2^+ electronic stopping ratio as a function of the logarithm of dwell time τ at different incident ion velocities. It can be seen that at longer dwell times the stopping ratio tends to 1 while at early times the ratio is larger than 1. This is because the two protons in the early stages are very close and they feel greater vicinage forces while in the last stages the protons are completely separated out and travel as isolated ions. When target electron collisions are included in calculations, they contribute to a great extend to increase the energy loss of the fragmented H_2^+ ion at all velocities. The stopping ratio increment is more noticeable at early dwell times while for longer times the stopping ratio tend to the same value than when the collisions are not included. This increment is more prominent for lower velocities due to vicinage forces in z direction, i.e., the sum $F_z(z) + F_z(-z)$ is more negative for lower velocities.

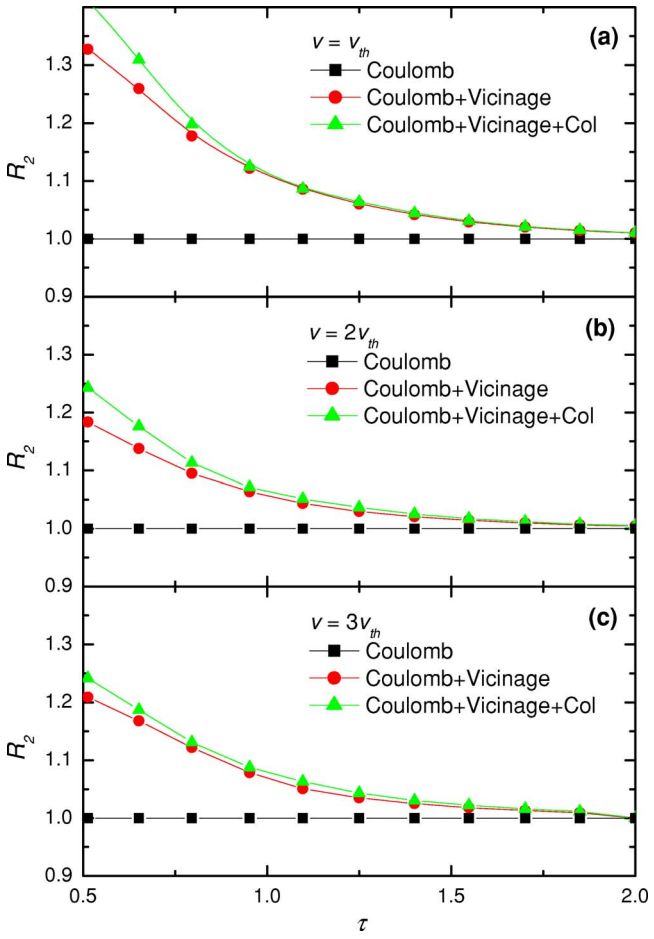

FIG. 6. (Color online) H_2^+ electronic stopping ratio R_2 as a function of the logarithm of dwell time τ when the initial azimuthal angle is $\alpha_0 = 60°$; for the same conditions as in Fig. 4.

V. CONCLUSIONS

In this work, the effects of target electron-electron collisions in the correlated motion of the fragmented H_2^+ protons has been deeply examined. Specifically the target is deuterium in a plasma state with temperature $T_e = 10$ eV and density $n = 10^{23}$ cm^{-3}. The correlated motion of the two protons is due to Coulomb and vicinage forces between them. It has been checked that vicinage forces always screen out Coulomb explosions of the fragmented H_2^+ protons. This screening is consequence of the asymmetry of the vicinage forces obtained in Sec. III that approaches the two protons. It results in decreasing the interproton distance r and delaying Coulomb explosion. Vicinage forces also tend to align the interproton vector in the motion direction. Finally it has been seen that they increase the correlated H_2^+ stopping at early times decreasing to the stopping of two isolated protons value at longer dwell times.

Nevertheless these vicinage effects can be modified by target electron-electron collisions. These collisions can enhance the calculated self-stopping force over the collisionless results. For protons with velocities $v = 2.5v_{\text{th}}$, the self-stopping force is increased by 11% and the modulus of the proton vicinage force also increases by 15% (at $\sigma = 0$) for this

particular plasma target. Concerning the correlated motion of the two protons, the target electron-electron collisions do not cause many changes in the evolution of the interproton distance, only small differences are seen for the slowest velocity $v_p = v_{\text{th}}$. But these collisions make that the interproton vector angle, α, with the motion direction overaligns for slower proton velocities while misaligns for faster ones. Finally these collisions contribute to a great extend to increase the energy loss of the fragmented H_2^+ ion at all velocities. The energy loss increment is more noticeable at early dwell times while for longer times the energy loss tend to the same value than when target electron collisions are not included. The main conclusion of this work is that correlated motion of charged particles cannot be studied realistically without considering the effects of target electron-electron collisions.

ACKNOWLEDGMENTS

This work was financed by the Spanish Ministerio de Educación y Cultura.

[1] V. Malka, S. Fritzler, E. Lefebvre, M.-M. Aleonard, F. Burgy, J.-P. Chambaret, J.-F. Chemin, K. Krushelnick, G. Malka, S. P. D. Mangles, Z. Najmudin, M. Pittman, J.-P. Rousseau, J.-N. Scheurer, B. Walton, and A. E. Dangor, Science **298**, 1596 (2002).

[2] E. L. Clark, K. Krushelnick, J. R. Davies, M. Zepf, M. Tatarakis, F. N. Beg, A. Machacek, P. A. Norreys, M. I. K. Santala, I. Watts, and A. E. Dangor, Phys. Rev. Lett. **84**, 670 (2000).

[3] R. Kodama, K. A. Tanaka, Y. Sentoku, T. Matsushita, K. Takahashi, H. Fujita, Y. Kitagawa, Y. Kato, T. Yamanaka, and K. Mima, Phys. Rev. Lett. **84**, 674 (2000).

[4] R. A. Snavely, M. H. Key, S. P. Hatchett, T. E. Cowan, M. Roth, T. W. Phillips, M. A. Stoyer, E. A. Henry, T. C. Sangster, M. S. Singh, S. C. Wilks, A. MacKinnon, A. Offenberger, D. M. Pennington, K. Yasuike, A. B. Langdon, B. F. Lasinski, J. Johnson, M. D. Perry, and E. M. Campbell, Phys. Rev. Lett. **85**, 2945 (2000).

[5] M. Roth, A. Blazevic, M. Geissel, T. Schlegel, T. E. Cowan, M. Allen, J.-C. Gauthier, P. Audebert, J. Fuchs, J. Meyer-ter-Vehn, M. Hegelich, S. Karsch, and A. Pukhov, Phys. Rev. ST Accel. Beams **5**, 061301 (2002).

[6] M. Hegelich, S. Karsch, G. Pretzler, D. Habs, K. Witte, W. Guenther, M. Allen, A. Blasevic, J. Fuchs, J. C. Gauthier, M. Geissel, P. Audebert, T. Cowan, and M. Roth, Phys. Rev. Lett. **89**, 085002 (2002).

[7] G. Basbas and R. H. Ritchie, Phys. Rev. A **25**, 1943 (1982).

[8] N. R. Arista and A. Gras-Marti, J. Phys.: Condens. Matter **3**, 7931 (1991).

[9] M. Vicanek, I. Abril, N. R. Arista, and A. Gras-Marti, Phys. Rev. A **46**, 5745 (1992).

[10] J. D'Avanzo, M. Lontano, and P. F. Bortignon, Phys. Rev. A **45**, 6126 (1992).

[11] C. Deutsch, Phys. Rev. E **51**, 619 (1995).

[12] C. Deutsch and N. A. Tahir, Phys. Fluids B **4**, 3735 (1992).

[13] S. Eliezer, J. M. Martinez-Val, and C. Deutsch, Laser Part. Beams **13**, 43 (1995).

[14] J. Neufeld and R. H. Ritchie, Phys. Rev. **98**, 1632 (1955).

[15] A. Selchow and K. Morawetz, Phys. Rev. E **59**, 1015 (1999); **69**, 039902(E) (2004).

[16] E. Fermi, Phys. Rev. **57**, 485 (1940).

[17] J. Lindhard, K. Dan. Vidensk. Selsk. Mat. Fys. Medd. **28**, 1 (1954).

[18] J. Lindhard and A. Winther, K. Dan. Vidensk. Selsk. Mat. Fys. Medd. **34**, 1 (1964).

[19] G. Zwicknagel, C. Toepffer, and P. G. Reinhard, Phys. Rep. **309**, 117 (1999).

[20] N. D. Mermin, Phys. Rev. B **1**, 2362 (1970).

[21] M. D. Barriga-Carrasco, G. Maynard, and Yu. K. Kurilenkov, Phys. Rev. E **70**, 066407 (2004).

[22] R. Garcia-Molina and M. D. Barriga-Carrasco, Phys. Rev. A **68**, 054901 (2003).

[23] M. D. Barriga-Carrasco and G. Maynard, Laser Part. Beams **23**, 211 (2005).

[24] T. Peter and J. Meyer-ter-Vehn, Phys. Rev. A **43**, 1998 (1991).

[25] L. Spitzer, *Physics of Fully Ionized Gases* (Interscience, New York, 1961).

[26] M. D. Barriga-Carrasco and R. Garcia-Molina, Phys. Rev. A **68**, 062902 (2003).

[27] N. R. Arista, Nucl. Instrum. Methods Phys. Res. B **164–165**, 108 (2000).